A Genetically Engineered Anti-CD45 Single-Chain Antibody-Streptavidin Fusion Protein for Pretargeted Radioimmunotherapy of Hematologic Malignancies

Yukang Lin,[1] John M. Pagel,[1,2] Donald Axworthy,[3] Anastasia Pantelias,[1] Nathan Hedin,[1] and Oliver W. Press[1,2]

[1]The Fred Hutchinson Cancer Research Center; [2]Division of Oncology, University of Washington School of Medicine; and [3]Aletheon Pharmaceuticals, Inc., Seattle, Washington

Abstract

Acute myelogenous leukemia (AML) currently kills the majority of afflicted patients despite combination chemotherapy and hematopoietic cell transplantation (HCT). Our group has documented the promise of radiolabeled anti-CD45 monoclonal antibodies (Ab) administered in the setting of allogeneic HCT for AML, but toxicity remains high, and cure rates are only 25% to 30% for relapsed AML. We now show the superiority of pretargeted radioimmunotherapy (PRIT) compared with conventional radioimmunotherapy using a recombinant tetravalent single-chain Ab-streptavidin (SA) fusion protein (scFv$_4$SA) directed against human CD45, administered sequentially with a dendrimeric N-acetylgalactosamine–containing clearing agent and radiolabeled 1,4,7,10-tetraazacyclododecane-N,N′,N″,N‴-tetraacetic (DOTA)-biotin. The scFv$_4$SA construct was genetically engineered by fusing Fv fragments of the human CD45-specific BC8 Ab to a full-length genomic SA gene and was expressed as a soluble tetramer in the periplasmic space of Escherichia coli. The fusion protein was purified to >95% homogeneity at an overall yield of ∼50% using iminobiotin affinity chromatography. The immunoreactivity and avidity of the fusion protein were comparable with those of the intact BC8 Ab, and the scFv$_4$SA construct bound an average of 3.9 biotin molecules out of four theoretically possible. Mouse lymphoma xenograft experiments showed minimal toxicity, excellent tumor-specific targeting of the fusion protein and radiolabeled DOTA-biotin in vivo, marked inhibition of tumor growth, and cured 100% of mice bearing CD45-expressing tumors. These promising results have prompted large-scale cGMP production of the BC8 fusion protein for clinical trials to be conducted in patients with hematologic malignancies. (Cancer Res 2006; 66(7): 3884-92)

Introduction

Acute myeloid leukemia (AML) afflicts 10,500 Americans annually, and 7,800 die of this malignancy each year, despite current therapies (1). High-dose chemoradiotherapy with hemato-poietic cell transplantation (HCT) is effective (2); however, only 20% to 30% of high-risk patients with advanced AML are cured due to both treatment-related mortality and leukemic relapse. Prior studies have shown that increasing doses of total body irradiation (TBI) from 12 to 15.75 Gy before HCT diminishes the relapse rate but increases treatment-related toxicity, nullifying the advantage of the lower relapse rate (3–5). Radioimmunotherapy is an emerging approach to increase the specific radiation dose delivered to malignant cells without increasing extramedullary toxicities and has produced promising results in AML and lymphoma trials (6–13). In AML patients undergoing HCT, radiolabeled antibodies (Ab) have been used as an adjuvant to TBI and chemotherapy and might reduce or eliminate the need for TBI (10, 11, 14, 15).

Anti-CD33 Ab have been most widely tested for AML therapy (12, 14, 16–18). However, in our trials using an ^{131}I-labeled anti-CD33 Ab, the low surface antigen expression resulted in a low percentage of radioisotope targeted to leukemic cells. Furthermore, the rapid internalization of the Ab-antigen complex and resultant metabolism and elimination of radiation from the tumor cells contributed to a suboptimal therapeutic result (14, 19). In recent years, we have focused on the CD45 antigen as an attractive alternative target for radioimmunotherapy of AML. CD45 is a ∼200-kDa tyrosine phosphatase that is stably expressed at a high density on the surface of virtually all hematopoietic cells except mature erythrocytes and platelets. Most hematologic malignancies, including 85% to 90% of acute lymphoid and myeloid leukemias, express CD45; however, CD45 is not found on nonhematopoietic tissues (20, 21). Available data suggest that CD45 is not shed into the bloodstream, is not rapidly internalized (19), and is expressed at a high surface density on the vast majority of leukemias and lymphomas (20). In clinical trials, our group has escalated ^{131}I-anti-CD45–radiolabeled Ab combined with chemotherapy to myeloablative levels and relied on HCT to reconstitute hematopoiesis (10, 11, 14, 15, 22). These studies have shown the safety and specificity of radiation targeting to hematopoietic tissues with very low relapse rates (15-20%) and excellent disease-free survival (60-65% at 5 years) in patients with AML in first remission. Although this approach is effective, the attendant toxicity is substantial, and the dose intensity of antileukemic radiation is limited by the radiation delivered to lung and liver. The doses of normal organ radiation exposure are at least partially due to the relatively long-circulating half-life of radiolabeled Ab in the blood.

We are currently testing a method of dose-intensified radio-immunotherapy called "pretargeting" radioimmunotherapy (PRIT) that might achieve improved outcomes with less toxicity. This method dissociates the slow distribution phase of the Ab molecule from the delivery of the therapeutic radionuclide (23–26). The tumor-reactive Ab is initially administered in a nonradioactive form.

After maximal accumulation of Ab in the tumor, a small radioactive moiety with high affinity for the tumor-reactive Ab is administered. Because of its small size, this second reagent penetrates tumors rapidly where the pretargeted Ab traps it. Unbound molecules of the radioactive reagent are rapidly cleared from the blood and excreted in the urine. As a further refinement, a clearing agent (CA) can be injected shortly before the radiolabeled small molecule to remove excess Ab from the bloodstream and prevent it from complexing with the radiolabeled small molecule (23, 27, 28). One of the most promising PRIT strategies exploits the high affinity (10^{-13} to 10^{-15} mol/L) of streptavidin (SA), a nonglycosylated 60-kDa homotetrameric protein from the bacterium *Streptomyces avidinii*, for biotin, a 244-Da complex aliphatic heterocycle. SA monomers contain one binding site for biotin per SA subunit.

A major improvement in PRIT technology involved enhancing the uniformity of the Ab-SA targeting molecule (29, 30). Schultz et al. developed a recombinant fusion protein consisting of an anti-CD20 scFv fused to SA and expressed in a soluble tetrameric form (172 kDa) in the periplasm of *Escherichia coli* (31). The scFv₄SA fusion protein maintained the full antigen and biotin binding capabilities of its parent molecules and was effective in pretargeting studies in mice. It was easier and less costly to manufacture and purify than Ab-SA chemical conjugates. *In vivo*, the scFv₄SA exhibited more rapid systemic clearance than the first-generation covalent whole Ab-SA conjugates, consistent with the lack of the Fc region of the Ab. However, the greater molecular weight of the scFv₄SA tetramer (~172 kDa) prevented direct renal elimination via glomerular filtration, and the absence of the Fc region minimized uptake in tissues containing Fc receptors (32). In PRIT protocols employing a biotinylated *N*-acetylgalactosamine CA, excess scFv₄SA could be quantitatively eliminated from blood by hepatic clearance via asialoglycoprotein receptors before delivery of radiobiotin (23). Fusion constructs targeting CD25, EpCAM, and TAG72 have also been expressed and purified in high yield and have been the subject of significant preclinical work as well as several phase I clinical studies (27, 33–35).

In this report, we describe for the first time the genetic engineering, expression, purification, characterization, and *in vivo* testing of a novel anti-CD45 scFv₄SA fusion protein and show its promise for future clinical trials in patients with leukemia and lymphoma.

Materials and Methods

Cell culture. The human Ramos B lymphoma cell line (American Type Culture Collection, Bethesda, MD) and the BC8 hybridoma cell line were maintained in log phase growth in RPMI 1640 with 10% heat-inactivated FCS.

Purification of BC8 Ab. The murine BC8 (anti-hCD45) IgG1 Ab was produced in hollow fiber bioreactors in the Biologics Production Facility at the Fred Hutchinson Cancer Research Center (FHCRC, Seattle, WA) and purified by protein A immunoabsorption column chromatography (10, 15).

Construction of a BC8 anti-CD45 *scFv₄SA* fusion gene. The V_H and V_L fragments of the murine BC8 Ab were obtained by reverse transcription-PCR (RT-PCR) from the BC8 hybridoma cell line (American Type Culture Collection). The first-strand cDNAs for V_H and V_L were prepared by a reverse transcription reaction using oligonucleotides for the Ab constant regions (5′-TAGCTGGCGGCC GCTTTCTTGTCCACCTTGGTGC for V_H and 5′-TAGCTGGCGGCCGCCCTGTTGAAGCTCTTGACAAT for V_L). The DNA fragments of the variable regions were PCR amplified from cDNAs using the constant region primers and degenerate variable region primers (5′-TGCCGTGAATTCGTSMARCTGCAGSARTCWGG for V_H and 5′-TGCCGTGAATTCCATTSWGCTGACCARTCTC for V_L). The PCR fragments were cloned into the pCR 2.1 vector (Invitrogen, Carlsbad, CA), and variable regions of the BC8 Ab were delineated by DNA sequencing. The heavy-chain fragment was subcloned by PCR and then digested with *Nco*I-*Bgl*II and cloned into the vector pEX94B (36) previously digested with *Nco*I-*Bgl*II. The light chain was also subcloned by PCR, digested with *Xho*I-*Sst*I, and cloned into the pEX94B vector containing the BC8 V_H fragment at sites of *Xho*I-*Sst*I. A *Bgl*II-*Xho*I fragment containing a 25-mer gly₄ser linker was inserted to produce the E103-10 plasmid, containing the BC8 V_H/V_L *scFvSA* gene (Fig. 1*A-D*). A *Hin*dIII fragment (1.5 kb) of a bacterial chaperone *FKPA* gene (37) was cloned by PCR from *E. coli* genomic DNA (XL1-blue; Stratagene, La Jolla, CA) using the following pairs of oligos: (*a*) RX1230, 5′-GGATCCAAGCTTACGATCACGGTCATGAACACG and (*b*) RX1232,

Figure 1. Schematic of a BC8 *scFvSA* gene and characterization of its mature, tetravalent fusion protein. *A,* the *scFvSA* gene is composed of the scFv of the murine IgG1 anti-CD45 BC8 Ab and SA. *B,* a schematic showing the tetravalent fusion protein that results from the spontaneous formation of a stable SA homotetramer after secretion to the periplasmic space of *E. coli. C,* SDS-PAGE analysis of unpurified and iminobiotin-purified BC8 scFv₄SA fusion protein. The mass of the intact fusion protein (177 kDa) and the monomer (44 kDa) are indicated on this SDS-PAGE gel (4-12% Tris-glycine; Invitrogen) stained with Coomassie blue. *Lane M,* migration of prestained standards (SeeBlue; Invitrogen). *Lanes 1* and *2,* microfluidized and loaded *E. coli* crude lysate, respectively, containing BC8 scFv₄SA fusion protein. *Lanes 3* and *4,* flow-through and wash fractions, respectively, of an imino-purification column. *Lanes 5* and *6,* iminobiotin-purified fusion protein either without boiling (*lane 5*) or denatured by boiling for 5 minutes (*lane 6*). *D,* a separate SDS-PAGE gel was blotted onto a polyvinylidene difluoride membrane (Invitrogen) and probed with a goat anti-SA polyclonal Ab followed by an horseradish peroxidase–conjugated rabbit anti-goat IgG Ab and visualized with TMB substrate. Lanes are the same as in (*C*).
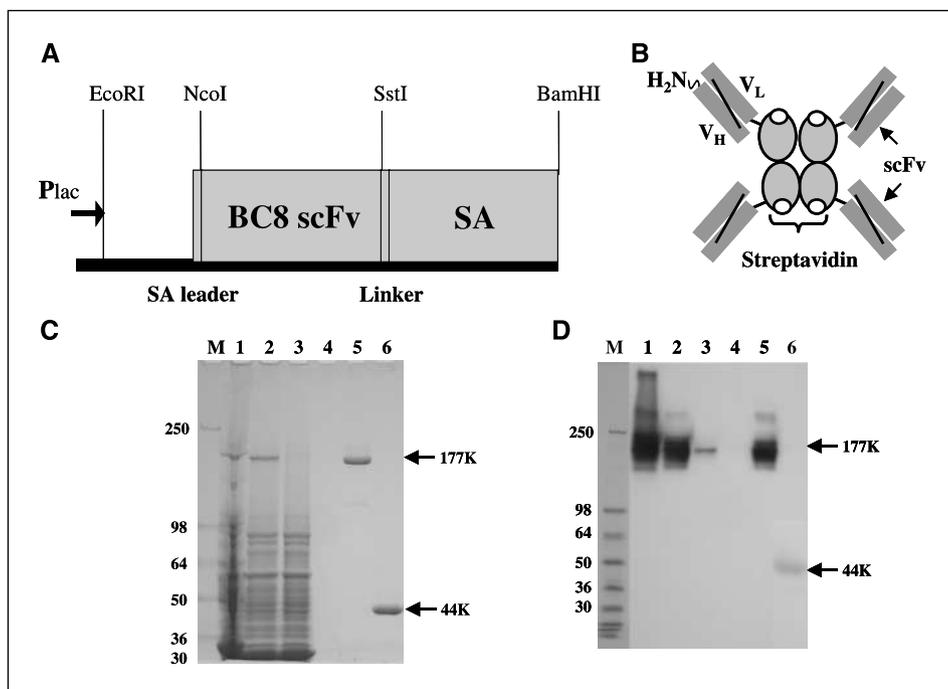
5′-CTCGAGAAGCTTTAACTAAATTAATACAGCGGA followed by digestion of the PCR fragment with *Hin*dIII, and inserted into E103-10 at a *Hin*dIII restriction site located downstream of the BC8 *scFvSA* gene. One clone with the *fkpA* chaperone gene in the same direction as the *scFvSA* gene was designated E121-3-10. Other clones containing different V_H/V_L configuration and linkers of various lengths or compositions were constructed in a similar fashion.

Expression and purification. *E. coli* strain XL1-Blue (Stratagene) was transformed with the BC8 scFvSA constructs, and transformants were grown in shaker flasks containing Terrific broth (Invitrogen) and carbenicillin (100 μg/mL) at 30°C. A single colony for each construct was checked for expression of fusion protein after induction with isopropyl-L-thio-B-D-galactopyranoside (IPTG) at a final concentration of 0.2 mmol/L (38). Periplasmic extracts were prepared and analyzed on a 4% to 20% Tris-glycine SDS-PAGE gel (Invitrogen) under nonreducing conditions. The E121-3-10/XL1-blue transformant was subsequently grown in a 4-liter fermentor (BioFlo 3000, New Brunswick Scientific, Edison, NJ) using methods similar to those published by Schultz et al. (31). The culture was induced with 0.1 g IPTG and allowed to ferment overnight, and the cells were harvested by centrifugation after 44 hours. The cell paste was washed with PBS thrice, and 394 g cells were processed by iminobiotin column chromatography (31). The product was extensively dialyzed, filtered (0.2 μm; Millipore, Billerica, MA), treated with 20% DMSO for 2 hours to reduce aggregation, concentrated to 2.7 mg/mL using a YM30 membrane (Millipore), filter sterilized, formulated in 5% sorbitol, and stored at −80°C.

In vitro **characterization.** The fusion protein was analyzed by SDS-PAGE on 4% to 12% Tris-glycine gels (Invitrogen) under nonreducing conditions. For immunoblot analysis, the protein bands were transferred to a polyvinylidene difluoride membrane (Invitrogen), blocked with bovine serum albumin, exposed to goat anti-SA (Vector Laboratories, Burlingame, CA) and a peroxidase-conjugated F(ab′)$_2$ fragment of rabbit anti-goat IgG (Jackson ImmunoResearch, West Grove, PA), and visualized with TMB substrate (Vector Laboratories). Size exclusion high-performance liquid chromatography (HPLC) analysis was carried out on a Zorbax GF-250 column (9.4 × 250 mm, 4 μm; Agilent, Palo Alto, CA) with 20 mmol/L sodium phosphate/0.5 mol/L sodium chloride/15% DMSO (pH 6.8-7.0) as a mobile phase and A_{280} as a detection wavelength. The molecular weight of the fusion protein was determined by matrix-assisted laser desorption/ionization (MALDI) mass spectrometry done on an Applied Biosystems Voyager DE Pro MALDI time-of-flight mass spectrometer. Competitive immunoreactivity was done by flow cytometry by incubating 500,000 Ramos cells at 4°C for 1 hour with a mixture of 3 μg of FITC-labeled BC8 Ab and titered amounts of unlabeled BC8 fusion protein as a competing agent. Unlabeled BC8 Ab and unlabeled CC49 scFv$_4$SA were used as positive and negative controls. Cells were washed and fixed with 1% formaldehyde, and the fluorescence intensity was measured on a FACScan (Becton Dickinson Labware, Franklin Lakes, NJ). Immunoreactivity of BC8 scFv$_4$SA and BC8 Ab were also compared after radioiodinating with ^{125}I and assessing binding to target Ramos cells by the method of Lindmo et al. (39). Apparent binding avidity of ^{125}I-BC8 scFv$_4$SA and ^{125}I-BC8 Ab were compared by Scatchard analysis using previously published methods (40). Biotin binding capacity was determined by incubating the fusion protein (100 μL, 1-2 nmol/mL) with freshly diluted biotin-cyanocobalimin (10 μL, 2.16 mg/mL) and quantifying the amount of unbound biotin-cyanocobalimin by HPLC using an unbound biotin serial titration standard curve.

Synthesis of a BC8 Ab-SA chemical conjugate. Chemical conjugates of the BC8 Ab and SA were synthesized and purified as previously described (41, 42).

Blood clearance studies. Four normal BALB/c mice were coinjected with ^{125}I-labeled BC8 Ab (215 μg, 1.4 nmol i.p.) and ^{131}I-labeled BC8 scFv$_4$SA (250 μg, 1.4 nmol, i.p.) followed by serial retro-orbital blood sampling for 120 hours. A separate group of four mice was injected with ^{125}I-labeled 1.4 nmol BC8 scFv$_4$SA followed 20 hours later by biotinylated poly-GalNAc CA (50 μg, i.p.). Blood samples were gamma counted with correction for crossover of ^{131}I into the ^{125}I channel and for radioactive decay. The mean values and SDs were plotted, and areas under the curves (AUC) were calculated using GraphPad 4 Prism software (San Diego, CA).

Biodistribution studies. Female BALB/c nude mice (Animal Technologics, Kent, WA), ages 6 to 8 weeks, were maintained under protocols approved by the FHCRC Institutional Animal Care and Use Committee. Mice were injected with 1×10^7 Ramos cells s.c. in each flank to induce human lymphoma xenografts. Mice with similar tumor sizes (~100 mm^3) were selected for experimentation. Mice were placed on a biotin-free diet (Harlan Teklad, Madison, WI) for 5 days before experiments. Groups of five mice were injected i.p. with either 1.4 nmol of ^{125}I-labeled Ab (215 μg, 50 μCi), unlabeled Ab-SA (300 μg), or unlabeled BC8 scFv$_4$SA (250 μg) fusion protein, respectively. An escalated dose of the fusion protein was also studied (2.8 nmol, 500 μg). Mice in pretargeted groups received 1.4 nmol of BC8 Ab-SA or BC8 scFv$_4$SA and were injected i.p. 20 hours later with 5.8 nmol (50 μg) of a biotinylated *N*-acetylgalactosamine–containing CA. Mice that received 2.8 nmol of BC8 scFv$_4$SA were subsequently injected with 11.6 nmol (100 μg) of CA. CA was followed 4 hours later by i.p. delivery of 1.2 nmol (1 μg) of ^{111}In-1,4,7,10-tetraazacyclododecane-*N*,*N*′,*N*″,*N*‴-tetraacetic (DOTA)-biotin (50 μCi). Mice were bled from the retro-orbital venous plexus and euthanized, and tumors and normal organs (lungs, stomach, small intestine, colon, spleen, quadriceps muscle, kidneys, and liver) were excised 24 hours after injection of radioactivity. Organs and tumors were weighed and gamma counted for ^{125}I or ^{111}In activity. The percent injected dose of radioisotope per gram (% ID/g) of blood, tumor or organ was calculated (after correcting for radioactive decay using an aliquot of the injectate), as were the tumor-to-normal organ ratios of absorbed radioactivity. Previous studies comparing the i.p. and i.v. injection routes showed identical biodistribution results after the first 6 hours. The mean values and SDs were plotted to generate time-activity curves. Control groups were injected with ^{111}In-DOTA-biotin alone or the nonbinding fusion protein CC49 scFv$_4$SA (2.8 nmol, 500 μg) followed by CA and ^{111}In-DOTA-biotin.

Therapy studies. Comparisons of directly labeled BC8 Ab and pretargeted BC8 scFv$_4$SA fusion protein were conducted using groups of 8 to 10 Ramos tumor-bearing mice to assess differences in therapeutic efficacy. Mice in groups that received directly labeled BC8 Ab were injected i.v. via the tail vein with 1.4 nmol DOTA-BC8 Ab labeled with either 200 or 400 μCi of ^{90}Y. Mice that received PRIT were injected i.v. via the tail vein with either 1.4 or 2.8 nmol of BC8 scFv$_4$SA fusion protein followed 20 hours later by 5.8 or 11.6 nmol, respectively, of CA. Four hours after CA injections, 1.2 nmol of DOTA-biotin labeled with 800 or 1,200 μCi of ^{90}Y was administered. CC49 scFv$_4$SA was used as a nonbinding control fusion protein followed by 5.8 nmol of CA and 1,200 μCi of ^{90}Y-DOTA-biotin. All mice were monitored every other day for general appearance, weight change, and tumor volume. Mice were euthanized if tumors caused discomfort and impaired ambulation, or if mice lost 25% of their starting weight.

Results

Design of an Anti-CD45 *scFvSA* gene construct. The DNA fragments encoding the immunoglobulin variable regions of the BC8 Ab were cloned by RT-PCR from BC8 hybridoma cells expressing the murine IgG1 Ab recognizing the human CD45 antigen. An scFv fragment, made from V_H and V_L cDNAs (Fig. 1*A*), was inserted to the full-length *SA* gene of *S. avidinii* between its leader and mature protein coding sequences with the *scFv* gene fused in-frame with the *SA* gene. The initial construct (E103-10) was designed to yield a soluble, homotetrameric fusion protein when expressed in the oxidizing environment of the *E. coli* periplasmic space, enabling intramolecular disulfide bond formation (Fig. 1*B*). The *scFvSA* gene encodes a mature protein of 426 amino acids (Fig. 2) with a calculated monomeric weight of M_r 44,338 Da and tetrameric weight of 177,353 Da. A bacterial chaperone gene (*fkpA*) was introduced into the plasmid (E121-3-10) to enhance fusion protein expression.

Fusion protein expression and purification. Several genetic variants of the BC8 fusion protein were constructed, which differed in linker length and the order of variable regions. All constructs were

analyzed first in shaker flasks for fusion protein expression as qualitatively determined on Coomassie blue–stained SDS-PAGE gels using boiled samples to analyze monomers and unboiled, non-reduced samples for tetramers. A 25-mer linker between the V_H and

V_L domains of *scFvSA* resulted in a 50% higher expression level than employing 15-mer linkers, and coexpression with the FkpA chaperone protein (e.g., E121-3-10 construct) tripled fusion protein expression. Substitution of a kanamycin resistance drug selection

```
1      CAGGTTCAGCTGGTGGAATCAGGAGGTGGCCTGGTGCAGCCTGGAGGATCCCTGAAACTC
1       Q   V   Q   L   V   E   S   G   G   G   L   V   Q   P   G   G   S   L   K   L

61     TCCTGTGCAGCCTCAGGATTCGATTTCAGTAGATACTGGATGAGTTGGGTCCGGCAGGCT
21      S   C   A   A   S   G   F   D   F   S   R   Y   W   M   S   W   V   R   Q   A

121    CCAGGGAAAGGGCTAGAATGGATTGGAGAGATTAATCCAACTAGCAGTACGATAAACTTT
41      P   G   K   G   L   E   W   I   G   E   I   N   P   T   S   S   T   I   N   F

181    ACGCCATCTCTAAAGGATAAAGTCTTCATCTCCAGAGACAACGCCAAAAATACGCTGTAC
61      T   P   S   L   K   D   K   V   F   I   S   R   D   N   A   K   N   T   L   Y

241    CTGCAAATGAGCAAAGTGAGATCCGAGGACACAGCCCTTTATTACTGTGCAAGAGGGAAC
81      L   Q   M   S   K   V   R   S   E   D   T   A   L   Y   Y   C   A   R   G   N

301    TACTATAGGTACGGAGATGCTATGGACTACTGGGGTCAAGGAACCTCAGTCACCGTGAGC
101     Y   Y   R   Y   G   D   A   M   D   Y   W   G   Q   G   T   S   V   T   V   S

361    AAGATCTCTGGTGGCGGTGGCTCGGGCGGTGGTGGGTCGGGTGGCGGCGGCTCGGGTGGT
121     K   I   S   G   G   G   G   S   G   G   G   G   S   G   G   G   G   S   G   G

421    GGTGGGTCGGGCGGCGGCGGCTCGAGCGACATCGTGCTGACCCAGTCTCCTGCTTCCTTA
141     G   G   S   G   G   G   G   S   S   D   I   V   L   T   Q   S   P   A   S   L

481    GCTGTATCTCTGGGACAGAGGGCCACCATCTCATGCAGGGCCAGCAAAAGTGTCAGTACA
161     A   V   S   L   G   Q   R   A   T   I   S   C   R   A   S   K   S   V   S   T

541    TCTGGCTATAGTTATCTGCACTGGTACCAACAGAAACCAGGACAGCCACCCAAACTCCTC
181     S   G   Y   S   Y   L   H   W   Y   Q   Q   K   P   G   Q   P   P   K   L   L

601    ATCTATCTTGCATCCAACCTAGAATCTGGGGTCCCTGCCAGGTTCAGTGGCAGTGGGTCT
201     I   Y   L   A   S   N   L   E   S   G   V   P   A   R   F   S   G   S   G   S

661    GGGACAGACTTCACCCTCAACATCCATCCTGTGGAGGAGGAGGATGCTGCAACCTATTAC
221     G   T   D   F   T   L   N   I   H   P   V   E   E   E   D   A   A   T   Y   Y

721    TGTCAGCACAGTAGGGAGCTTCCATTCACGTTCGGCTCGGGGACAAAGTTGGAAATAAAG
241     C   Q   H   S   R   E   L   P   F   T   F   G   S   G   T   K   L   E   I   K

781    AGCTCTGGCTCTGGTTCGGCAGACCCCTCCAAGGACTCGAAGGCCCAGGTCTCGGCCGCC
261     S   S   G   S   G   S   A   D   P   S   K   D   S   K   A   Q   V   S   A   A

841    GAGGCCGGCATCACCGGCACCTGGTACAACCAGCTCGGCTCGACCTTCATCGTGACCGCG
281     E   A   G   I   T   G   T   W   Y   N   Q   L   G   S   T   F   I   V   T   A

901    GGCGCCGACGGCGCCCTGACCGGAACCTACGAGTCGGCCGTCGGCAACGCCGAGAGCCGC
301     G   A   D   G   A   L   T   G   T   Y   E   S   A   V   G   N   A   E   S   R

961    TACGTCCTGACCGGTCGTTACGACAGCGCCCCGGCCACCGACGGCAGCGGCACCGCCCTC
321     Y   V   L   T   G   R   Y   D   S   A   P   A   T   D   G   S   G   T   A   L

1021   GGTTGGACGGTGGCCTGGAAGAATAACTACCGCAACGCCCACTCCGCGACCACGTGGAGC
341     G   W   T   V   A   W   K   N   N   Y   R   N   A   H   S   A   T   T   W   S

1081   GGCCAGTACGTCGGCGGCGCCGAGGCGAGGATCAACACCCAGTGGCTGCTGACCTCCGGC
361     G   Q   Y   V   G   G   A   E   A   R   I   N   T   Q   W   L   L   T   S   G

1141   ACCACCGAGGCCAACGCCTGGAAGTCCACGCTGGTCGGCCACGACACCTTCACCAAGGTG
381     T   T   E   A   N   A   W   K   S   T   L   V   G   H   D   T   F   T   K   V

1201   AAGCCGTCCGCCGCCTCCATCGACGCGGCGAAGAAGGCCGGCGTCAACAACGGCAACCCG
401     K   P   S   A   A   S   I   D   A   A   K   K   A   G   V   N   N   G   N   P

1261   CTCGACGCCGTTCAGCAGTAA
421     L   D   A   V   Q   Q   *
```

Figure 2. DNA sequence of BC8 *scFvSA* fusion construct and its encoded amino acid sequence. The V_H (amino acids 1-120) and V_L (amino acids 150-260) fragments of anti-CD45 BC8 Ab were joined by a 25-mer linker (*first underline*) to form an scFv fragment that was subsequently fused to a full-length genomic SA (amino acids 267-426) by a second linker (*second underline*). The numbers on the left indicated the beginning of DNA and amino acid sequences for a mature BC8 scFv₄SA fusion protein.
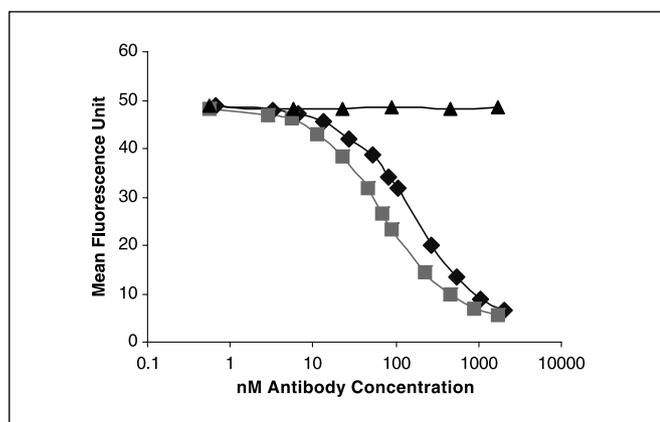
Figure 3. Competitive immunoreactivity assay. Serial dilutions of Ab BC8 (♦) or scFv$_4$SA (■) were competed with fluorescein-labeled BC8 Ab for binding to CD45-positive human Ramos lymphoma cells. An anti-Tag-72 CC49 scFv$_4$SA fusion protein (▲) serves as a negative control for the titration.

marker for the ampicillin resistance gene reduced expression by 40%. Although a mutation (H187S) in the light chain of the BC8 *scFvSA* created by site-specific mutagenesis increased the fusion protein expression in the shaker flask, the amino acid change in the complementary determining region of the V$_L$ seemed to affect the affinity of the Ab. Therefore, these constructs were not tested further. The E121-3-10 construct with a 25-mer Gly$_4$Ser scFv linker in the V$_H$-V$_L$ orientation expressed at 143 mg/L in a 4-liter fermentor. It was purified from homogenized cell extracts with a 72% yield on a single iminobiotin affinity column with a 50% overall purification yield. This iminobiotin-purified protein was analyzed for protein characterization, immunoreactivity, biotin-binding ability, blood clearance rate, *in vivo* tumor targeting, and *in vivo* therapy.

Biochemical characterization. SDS-PAGE analysis confirmed 95% purity of the fusion protein after iminobiotin chromatography (Fig. 1*C*). The major protein band migrated at a position corresponding to a molecular weight of 177 kDa as predicted for the tetrameric protein. Additional minor bands were also detected by Western blotting, identifying minor isoforms (Fig. 1*D*). All bands resolved into a single species of $M_r \sim 44$ kDa when the fusion protein was denatured by boiling before electrophoresis, consistent with a single protein entity dissociable into a homogeneous, monomeric subunit. Size exclusion HPLC showed that the purified fusion protein exhibited a major peak (8.011 min) with a retention time appropriate for the tetramer and a minor peak (7.424 min) representing an aggregated species (26%) with a higher molecular weight (data not shown). Such aggregated species were reduced to 6% after the purified protein was treated with 15% DMSO and analyzed by size exclusion HPLC. MALDI mass spectroscopy established a molecular weight of 177,443 Da for the tetramer and 44,389 Da for the monomer, in close agreement with the calculated mass of 177,353 Da for the most abundant isoform of the tetramer and 44,338 for the monomer. Immunoreactivity was assessed by flow cytometry in a competitive assay with a fluorescence-labeled BC8 Ab for binding to the CD45-positive Ramos cell line. IC$_{50}$ values indicated that the tetravalent scFv$_4$SA fusion protein was twice as immunoreactive as the divalent BC8 Ab on a molar basis (Fig. 3). More precise quantification of the immunoreactivity and avidity of the fusion protein was obtained by radioiodinating and testing binding at various concentrations to target cells using Lineweaver-Burke and Scatchard cell binding assays (31, 39). These tests
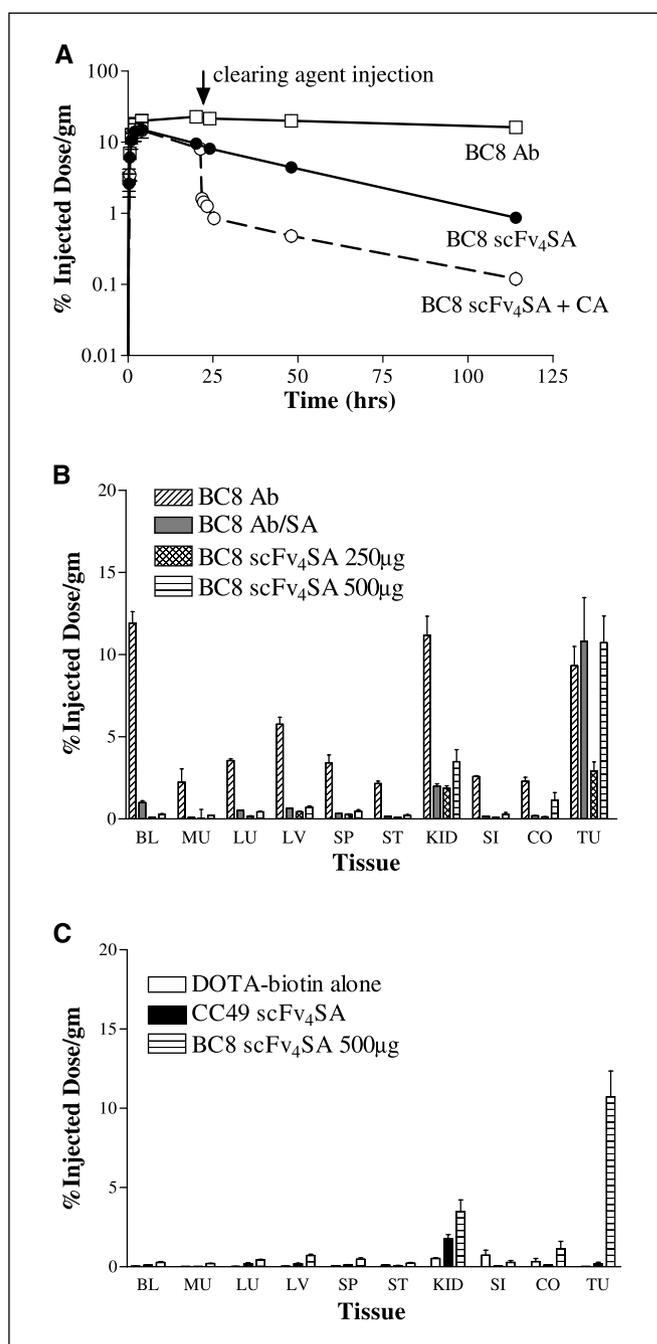

Figure 4. Comparative pharmacokinetics and biodistributions of radiolabeled BC8 Ab and of ^{111}In-DOTA-biotin pretargeted with the BC8 scFv$_4$SA fusion protein. *A,* whole blood clearance of ^{125}I-labeled BC8 Ab (215 μg, 1.4 nmol i.p.) and ^{131}I-labeled BC8 scFv$_4$SA (250 μg, 1.4 nmol i.p.) with or without biotinylated poly-GalNAc CA treatment (50 μg i.p.) in normal BALB/c mice (*n* = 4 per group). The CA was injected 20 hours after the labeled fusion protein. *B,* the biodistribution of ^{125}I-labeled BC8 whole Ab or pretargeted ^{111}In-DOTA-biotin in athymic mice bearing Ramos human lymphoma xenografts (*n* = 5 per group). ^{125}I-labeled BC8 whole Ab (215 μg, 1.4 nmol), BC8 Ab-SA conjugate (300 μg, 1.4 nmol), or BC8 scFv$_4$SA fusion protein (250 μg, 1.4 nmol or 500 μg, 2.8 nmol) was injected i.p. at *t* = 0 hour. CA (50 μg) was administered i.p. at *t* = 20 hours and ^{111}In-DOTA-biotin (1.0 μg i.p.) at *t* = 24 hours to pretargeted groups. Mice were sacrificed 24 hours after injection of radioactivity. *C,* ^{125}I-labeled anti-TAG-72 fusion protein (CC49 scFv$_4$SA, 500 μg) or anti-CD45 fusion protein (BC8 scFv$_4$SA, 500 μg) was injected i.p. at *t* = 0 hour followed by CA and ^{111}In-DOTA-biotin as above. Mice were sacrificed 24 hours after injection of radioactivity. *Columns/points,* mean; *bars,* SD. *BL,* blood; *MU,* muscle; *LU,* lung; *LV,* liver; *SP,* spleen; *ST,* stomach; *KID,* kidney; *SI,* small intestine; *CO,* colon; and *TU,* tumor.

confirmed full retention of immunoreactivity and avidity by the scFv₄SA fusion protein compared with the BC8 Ab. Two separate immunoreactivity experiments showed immunoreactivity (83%, Ramos cells; 59%, Raji cells) equivalent to that of the parent BC8 Ab (80%, Ramos; 58%, Raji). The avidity of the fusion protein (K_a = $2.76 \pm 0.18 \times 10^8$ L/mol for Ramos cells and $2.42 \pm 0.12 \times 10^8$ L/mol for Raji cells) was slightly superior to that of the Ab (K_a = $2.28 \pm 0.14 \times 10^8$ L/mol for Ramos cells and $1.93 \pm 0.15 \times 10^8$ L/mol for Raji cells), presumably due to its tetravalency. The biotin binding capacity assessed by a cyanocobalimin-biotin HPLC assay revealed an average of 3.9 of 4 possible biotin-binding sites per fusion protein molecule.

Blood clearance and biodistributions. Blood clearance studies in BALB/c mice showed more rapid disappearance of the BC8 scFv₄SA fusion protein than of the BC8 Ab, consistent with other fusion proteins (Fig. 4*A-C*). AUC calculations showed a 2-fold faster clearance of the fusion protein than of the Ab (AUC = 3,908 versus 6,833 pmol/mL, respectively). A single i.p. injection of a biotinylated poly(GalNAc) CA caused a >10-fold decrease in fusion protein concentration within 1 hour. Next, the BC8 fusion protein was assessed for its ability to localize radioactivity to tumor sites in athymic mice bearing human lymphoma (Ramos) xenografts. Initial experiments were conducted with equimolar doses (1.4 nmol) of fusion protein, BC8 Ab-SA chemical conjugate, and intact whole BC8 Ab. An escalated dose (2.8 nmol) of the fusion protein was also compared with compensate for the 2-fold more rapid clearance of the fusion protein from the circulation. ^{125}I-labeled BC8 whole Ab (1.4 nmol, 215 μg), unlabeled BC8 Ab-SA chemical conjugate (1.4 nmol, 300 μg), or unlabeled BC8 scFv₄SA fusion protein (1.4 nmol, 250 μg and 2.8 nmol, 500 μg) were injected i.p. at *t* = 0 hour. In the pretargeted groups, CA (5.8 or 11.6 nmol, 50 or 100 μg) was injected i.p. at *t* = 20 hours, and ^{111}In-labeled DOTA-biotin (1.2 nmol, 1 μg, 50 μCi) was injected i.p. at *t* = 24 hours. The concentration of the ^{125}I-BC8 Ab remained high in well-perfused soft tissues (e.g., 5.7% ID/g in the liver) 24 hours after injection in the conventional radio-immunotherapy group, as expected from the high concentrations in blood (11.8% ID/g; Fig. 4*B*). In contrast, the concentrations of ^{111}In-labeled DOTA-biotin in groups pretargeted with either the BC8 Ab-SA chemical conjugate or the BC8 scFv₄SA fusion protein were very low in blood (0.2-1.1% ID/g) and in normal organs (e.g., 0.4-0.7%

ID/g in the liver after 24 hours). High concentrations of ^{111}In-DOTA-biotin were stably delivered to Ramos tumors with pretargeting methods (10.8% ID/g with 1.4 nmol BC8 Ab-SA chemical conjugate and 10.7% ID/g with 2.8 nmol scFv₄SA fusion protein after 24 hours). Increasing the dose of the pretargeted fusion protein improved the retention of labeled biotin bound to the fusion protein in tumor tissue, from 2.9% ID/g after 24 hours with 1.4 nmol BC8 scFv₄SA to 10.7% ID/g with 2.8 nmol. The normal organ with the highest content of ^{111}In in pretargeted groups was the kidney, presumably due to renal excretion of this small moiety. Tumor-to-blood ratios of radioactivity using pretargeted BC8 scFv₄SA (2.8 nmol) reached 46:1 after 24 hours compared with 7:1 with the BC8 Ab-SA chemical conjugate and only 0.8:1 with the directly labeled BC8 Ab (Table 1). Liver uptake of control ^{111}In-DOTA-biotin alone was minimal (0.72% ID/g at 24 hours; Fig. 4*C*), indicating that scFv₄SA-CA complexes were efficiently internalized after hepatic clearance, rendering them inaccessible to subsequently administered radiolabeled biotin. The CC49 scFv₄SA fusion protein, which recognizes the tumor-associated glycoprotein 72 antigen, which is not present on Ramos cells, was used as a negative control (Fig. 4*C*). The % ID/g of ^{111}In-DOTA-biotin pretargeted by the CC49 fusion protein were similar in nontumor tissues (0.5-1.7% ID/g) to those seen in mice injected with BC8 scFv₄SA (0.1-2.0% ID/g), showing the absence of antigen-mediated uptake in normal mouse tissues of either fusion construct. No significant binding of ^{111}In-DOTA-biotin was detected in tumors after administration of CC49 scFv₄SA fusion protein (0.19% ID/g of tumor). Ratios of tumor-to-blood 24 hours after injection of radioactivity were ∼32 to 46:1 for the BC8 fusion protein groups versus 1.9:1 for the CC49 scFv₄SA group (Table 1).

Radioimmunotherapy with directly labeled BC8 Ab compared with PRIT using BC8 scFv₄SA fusion protein. The therapeutic efficacy of conventional radioimmunotherapy using ^{90}Y-DOTA-BC8 Ab was compared with the efficacy of pretargeted ^{90}Y-DOTA-biotin following administration of BC8 scFv₄SA in athymic mice bearing palpable tumor xenografts (∼100 mm³). Groups of 8 to 10 animals each were either observed untreated or injected i.v. with either 200 or 400 μCi of directly labeled ^{90}Y-DOTA-BC8 Ab or with 800 or 1,200 μCi of pretargeted ^{90}Y-DOTA-biotin 4 hours after administration of CA and 24 hours after administration

Table 1. Tumor-to-normal organ ratios using conventional radioimmunotherapy with 1.4 nmol ^{125}I-BC8 Ab or PRIT with ^{111}In-DOTA-biotin following BC8 antibody-SA (chemical conjugate) or BC8 scFv₄SA fusion protein (1.4 or 2.8 nmol) 24 hours after the injection of radioactivity

Organ	BC8 Ab	BC8 Ab-SA	BC8 scFv₄SA (1.4 nmol)	BC8 scFv₄SA (2.8 nmol)
Blood	0.78 ± 0.20	6.57 ± 2.32	32.29 ± 10.56	45.83 ± 21.41
Kidney	0.84 ± 0.27	5.33 ± 2.88	1.57 ± 0.63	2.19 ± 0.33
Liver	1.66 ± 0.55	13.12 ± 9.41	7.17 ± 3.21	14.76 ± 1.48
Lung	2.43 ± 0.70	16.48 ± 12.85	22.54 ± 7.51	24.36 ± 4.35
Muscle	5.88 ± 3.72	118.77 ± 92.46	76.74 ± 19.72	53.21 ± 19.45
Small intestine	3.65 ± 1.08	56.81 ± 48.54	34.07 ± 11.02	73.12 ± 59.93
Colon	4.13 ± 1.14	43.72 ± 32.35	25.45 ± 14.95	14.07 ± 8.10
Spleen	2.79 ± 0.69	25.30 ± 18.91	10.99 ± 3.88	23.59 ± 5.48
Stomach	4.40 ± 1.37	51.45 ± 40.20	30.14 ± 11.03	53.16 ± 20.90

NOTE: For pretargeting groups, CA (5.8 nmol) was delivered 20 hours after Ab-conjugate or fusion protein administration followed 4 hours later by 1.2 nmol ^{111}In-biotin (50 μCi). Groups of five mice were used to generate mean values. Data were normalized for tissue weight and corrected for radioactive decay.

of 1.4 or 2.8 nmol BC8 scFv$_4$SA or 1.4 nmol of CC49 scFv$_4$SA. Previous studies showed that doses of directly labeled ^{90}Y-labeled Ab >400 μCi were lethal in 100% of mice. Nine of 10 untreated control mice and six of nine animals treated with control CC49 scFv$_4$SA + 1200 μCi of ^{90}Y-DOTA-biotin exhibited exponential growth of lymphoma xenografts, necessitating euthanasia by day 15 (Fig. 5*A* versus *B*). All animals treated with 400 μCi of directly labeled ^{90}Y-DOTA-BC8 Ab displayed severe toxicity and lost ∼25% of body weight requiring euthanasia, despite initial tumor regression (Fig. 5*B*). Three of eight mice receiving 200 μCi of ^{90}Y-DOTA-BC8 Ab were euthanized due to severe toxicity (>25% weight loss), two achieved durable complete remissions, and three mice attained partial tumor remissions but eventually required euthanasia for progressive tumor growth. All nine animals treated with low-dose PRIT (1.4 nmol of BC8 scFv$_4$SA + 800 μCi of ^{90}Y-DOTA-biotin) experienced a decrease in tumor growth rate (four animals achieved complete tumor regressions or CR by day 23, but five mice experienced tumor regrowth requiring euthanasia; Fig. 5*A*). In contrast, treatment with the same amount of BC8 scFv$_4$SA followed by 1,200 μCi of ^{90}Y-DOTA-biotin resulted in six CRs, with the remaining three mice showing an initial decrease in tumor volume followed by regrowth. When the dose of BC8 scFv$_4$SA fusion protein was increased to 2.8 nmol, the number of CRs increased to 7 of 9 mice given 800 μCi of ^{90}Y-DOTA-biotin, and 9 of 9 mice with 1,200 μCi of ^{90}Y-DOTA-biotin (Fig. 5*B*). All nine mice in the latter group have survived >100 days without any tumor recurrences (Fig. 5*C*). Although long-term toxicity evaluations were not conducted in the current study, other pretargeting experiments have not shown any delayed toxicities even after 1 year of serial assessment of blood urea nitrogen, creatinine, transaminases, and histologic examination of kidney tissues at necropsy (43).

Discussion

AML kills 60% to 70% of affected adults despite improvements in induction chemotherapy and HCT. Several groups have documented the feasibility, safety, and efficacy of treating AML with radiolabeled anti-myeloid Ab, but studies to date have been limited by the low tumor-to-normal organ ratios of absorbed radiation attainable. Multistep pretargeting methods have been developed for other types of cancer and have shown marked improvements in the tumor-to-normal organ ratios of absorbed radiation achievable, as well as improved therapeutic results compared with conventional radioimmunotherapy (23, 27, 34, 44–46). In this article, we report for the first time the application of PRIT directed against an AML-associated antigen and describe five major findings. First, we show the feasibility of engineering, expressing, and purifying a fully functional tetravalent anti-CD45 scFv$_4$SA fusion protein that retains the immunoreactivity and avidity of the parent Ab and the full biotin binding capacity of the SA molecule. Second, we show that an *N*-acetylgalactosamine–containing dendrimeric CA can rapidly clear 90% to 98% of circulating fusion protein from the bloodstream by hepatic clearance within 30 minutes of CA administration. This clearance step seems critical because optimal tumor-to-normal organ ratios of radioactivity can only be achieved if trapping of radiobiotin by excess fusion protein circulating in the blood is minimized. Third, we show that all three components of the pretargeting system can be administered parenterally to mice with negligible toxicity. Fourth, we show specific delivery of high levels of radiation to tumor sites with minimal exposure of blood or normal organs to radiation. Finally, we document that delivery of
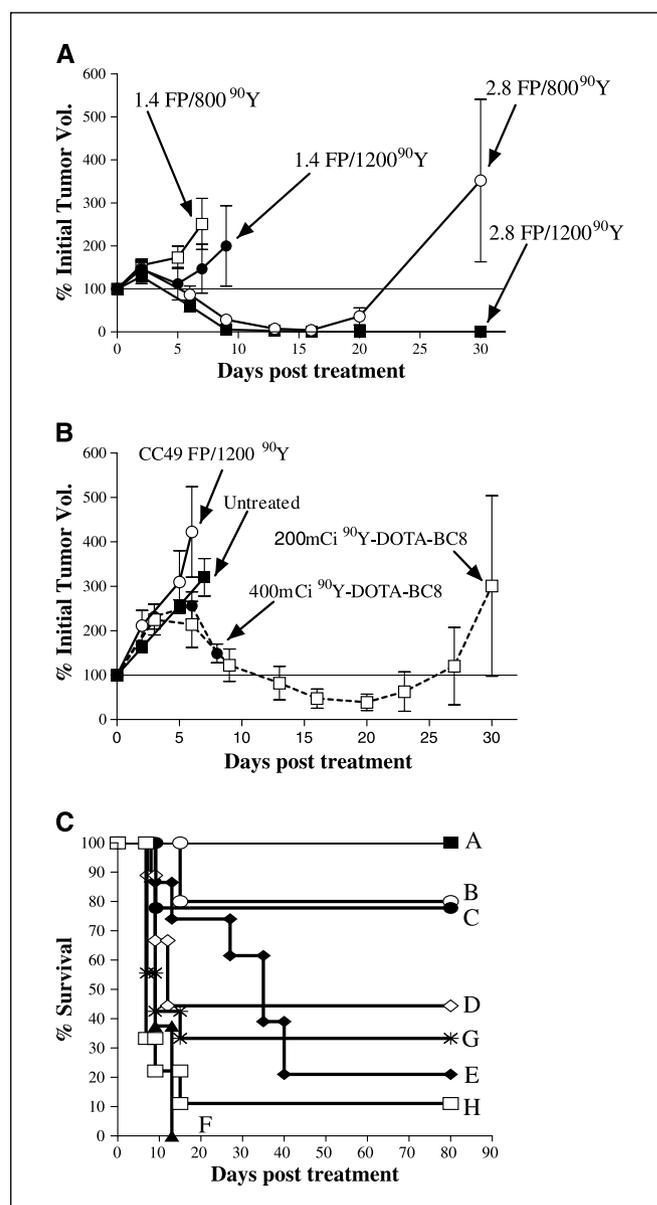

Figure 5. Therapeutic efficacy of PRIT using the BC8 scFv$_4$SA fusion protein compared with radioimmunotherapy using directly labeled ^{90}Y-DOTA-BC8 Ab. *A*, tumor growth was measured in athymic BALB/c mice bearing Ramos lymphoma xenografts injected i.v. with either 1.4 or 2.8 nmol of BC8 scFv$_4$SA fusion protein (*1.4 FP* or *2.8 FP*) followed 20 hours later with 5.8 or 11.6 nmol of CA, respectively, and 4 hours later with 800 or 1,200 μCi of ^{90}Y-DOTA-biotin. *B*, mice were injected with conventional radioimmunotherapy using 1.4 nmol of directly labeled ^{90}Y-DOTA-BC8 Ab with either 200 or 400 μCi of ^{90}Y. Control mice were either left untreated or given 1.4 nmol of CC49 scFv$_4$SA followed by 5.8 nmol of CA 20 hours later and 1,200 μCi of ^{90}Y-DOTA-biotin 24 hours after delivery of the fusion protein. Tumor growth is expressed as % initial tumor volume (*y axis*) measured over time (*x axis*). Curves were truncated in (*A*) and (*B*) when mice required euthanasia due to tumor progression or severe toxicity. *C*, Kaplan-Meier analysis of cumulative survival of mice bearing Ramos lymphoma xenografts treated with either directly labeled ^{90}Y-DOTA-BC8 Ab or PRIT using a BC8 scFv$_4$SA fusion protein. Groups of mice bearing Ramos tumor xenografts were treated as described in Fig. 4 legend and analyzed for survival as a function of time. Treatment groups included groups of nine mice treated with 2.8 nmol BC8 scFv$_4$SA and either 1,200 μCi (*A*) or 800 μCi (*B*) ^{90}Y-DOTA-biotin as well as groups of nine mice treated with 1.4 nmol BC8 scFv$_4$SA and either 1200 μCi (*C*) or 800 μCi (*D*) ^{90}Y-DOTA-biotin. Groups of eight mice were treated with either 200 μCi (*E*) or 400 μCi (*F*) of ^{90}Y-DOTA-BC8 Ab. As controls, groups of nine mice were either treated with 1.4 nmol of CC49 scFv$_4$SA and 1,200 μCi of ^{90}Y-DOTA-biotin (*G*) or left untreated (*H*). *FP,* fusion protein.

therapeutic doses of ^{90}Yttrium using BC8 scFv$_4$SA, but not a control fusion protein or a conventionally radiolabeled anti-CD45 Ab, can achieve durable remissions in all mice bearing CD45-expressing tumor xenografts.

Although some have expressed concerns about targeting an antigen expressed as broadly as CD45, important advantages also must be recognized. "Lineage-specific" radiolabeled Ab, such as those targeting CD45, may be superior to "leukemia-specific" radiolabeled Ab for patients in remission or in relapsed patients with subclinical involvement of extramedullary tissues, such as lymph nodes, because in these settings isolated malignant cells are surrounded by normal hematopoietic cells. Because the radiation from a radionuclide attached to an Ab bound to the surface of a cell can be emitted in any direction within a geographic area defined by the path length of the radionuclide, the isolated malignant cell may receive a significantly greater absorbed dose if the surrounding normal cells are targeted as well. We initially hypothesized that the superlative cell surface retention seen with the anti-CD45 Ab should make the CD45 antigen a particularly advantageous target for radioimmunotherapy (19). We partially validated this hypothesis by showing that ^{131}I-labeled anti-CD45 Ab target AML cells better and are retained longer than ^{131}I-anti-CD33 Ab and provide superior tumor targeting of AML xenografts in athymic mice (19). Furthermore, CD45 targeting permits therapy of a broad spectrum of malignancies, including myeloid leukemias, myelodysplasia, acute lymphoblastic leukemia, chronic lymphocytic leukemia, and both T- and B-cell lymphomas. One unavoidable consequence of CD45-targeted radioimmunotherapy, however, is that significant myelosuppression will almost always occur due to expression of CD45 on hematopoietic progenitor cells. Therefore, anti-CD45 radioimmunotherapy in humans may require HCT to restore hematopoiesis following eradication of the malignancy. Although this is a disadvantage, it is acceptable if cure rates are markedly improved. Furthermore, our group has documented the feasibility of HCT following anti-CD45 radioimmunotherapy in over 150 patients with myeloid malignancies (10, 11, 15).

Although we believe that the findings reported in this article are very encouraging, we acknowledge that there are some limitations. First, human target antigens (including CD45) are confined to tumor cells in xenograft systems. In contrast, in patients, CD45 is present on normal hematopoietic elements as well as tumor cells; consequently, toxicity profiles in the human may not be reliably mimicked. Second, the xenograft model, which facilitates measurement of tumor-to-normal organ ratios of absorbed radioactivity, consists of a single s.c. nodule analogous to a chloroma but is dissimilar from the disease pattern in most leukemia patients who have blood- and marrow-based disease. Finally, athymic and severe combined immunodeficient mice are severely immunodeficient, making it impossible to assess the role of the immune system in radioimmunotherapy using these models. The mouse xenograft model is thus an idealized situation that will not precisely mimic the human clinical situation. To address these concerns, we have begun experiments in syngeneic, immunocompetent murine

systems in which anti-murine CD45-SA conjugates are employed to pretarget radiobiotin to target cells in a setting where normal hematopoietic tissues also bind the conjugate. Preliminary findings indicate that CD45 PRIT is still effective in such a syngeneic setting.[4]

Several potential problems with the general concept of pretargeting must be acknowledged, including (*a*) its complexity, requiring multiple injections, (*b*) the presence of endogenous biotin which competes with radiolabeled biotin, (*c*) serum biotinidases, (*d*) the immunogenicity of SA, and (*e*) the relatively high doses of radiation delivered to the kidneys in some studies (35). Our previous studies and those of others have convinced us that the complexity of multiagent targeting and the presence of endogenous biotin and serum biotinidases are not serious impediments to the success of this approach (42, 44, 45, 47, 48). The immunogenicity of SA remains a significant issue that is being addressed by other investigators but is not a concern for our studies because we plan single dose therapy followed by HCT not repetitive cycles of therapy.

Despite the potential limitations mentioned above, we are convinced that PRIT will prove superior to conventional radioimmunotherapy because (*a*) PRIT improves the absolute amount of radioactivity deposited per gram of tumor, (*b*) accelerates the time frame for maximizing tumor uptake of radioactivity, (*c*) allows faster clearance of radioactivity from the circulation resulting in superior tumor-to-blood ratios, (*d*) permits target signal amplification because more than one radioactive biotin can bind to a tetravalent SA molecule, (*e*) causes less toxicity to normal organs, (*f*) minimizes the risk of radiolysis of Ab protein by high specific activity radionuclides, (*g*) may decrease the side effect profile by reducing the potential for serum complement fixation, and (*h*) enhances the feasibility of using radioisotopes of varying physical characteristics (β-emission energy and half-life). In view of these compelling advantages, we have initiated primate studies of CD45 pretargeting and begun production of the CD45 scFv$_4$SA fusion protein under cGMP conditions for human clinical trials in AML and non-Hodgkin's lymphoma.

Acknowledgments

---

[4] J. Pagel, in preparation.

References

1. Jemal A, Murray T, Ward E, et al. Cancer statistics, 2005. CA Cancer J Clin 2005;55:10–30.
2. Appelbaum FR. Allogeneic hematopoietic stem cell transplantation for acute leukemia. Semin Oncol 1997;24:114–23.
3. Clift RA, Buckner CD, Appelbaum FR, et al. Allogeneic marrow transplantation in patients with acute myeloid leukemia in first remission: a randomized trial of two irradiation regimens. Blood 1990;76:1867–71.
4. Clift RA, Buckner CD, Appelbaum FR, et al. Allogeneic marrow transplantation in patients with chronic myeloid leukemia in the chronic phase: a randomized trial of two irradiation regimens. Blood 1991;77:1660–5.
5. Clift RA, Buckner CD, Appelbaum FR, et al. Long-term follow-up of a randomized trial of two irradiation regimens for patients receiving allogeneic marrow transplants during first remission of acute myeloid leukemia. Blood 1998;92:1455–6.

6. Press OW, Eary JF, Appelbaum FR, et al. Radiolabeled-antibody therapy of B-cell lymphoma with autologous bone marrow support [see comments]. N Engl J Med 1993;329:1219–24.

7. Press OW, Eary JF, Appelbaum FR, et al. Phase II trial of ^{131}I-B1 (anti-CD20) antibody therapy with autologous stem cell transplantation for relapsed B cell lymphomas. Lancet 1995;346:336–40.

8. Press OW, Eary JF, Gooley T, et al. A phase I/II trial of iodine-131-tositumomab (anti-CD20), etoposide, cyclophosphamide, and autologous stem cell transplantation for relapsed B-cell lymphomas. Blood 2000;96:2934–42.

9. Juweid M, Sharkey RM, Markowitz A, et al. Treatment of non-Hodgkin's lymphoma with radiolabeled murine, chimeric, or humanized LL2, an anti-CD22 monoclonal antibody. Cancer Res 1995;55:5899–907s.

10. Matthews DC, Appelbaum FR, Eary JF, et al. Phase I study of (131)I-anti-CD45 antibody plus cyclophosphamide and total body irradiation for advanced acute leukemia and myelodysplastic syndrome. Blood 1999;94:1237–47.

11. Matthews DC, Appelbaum FR, Eary JF, et al. Development of a marrow transplant regimen for acute leukemia using targeted hematopoietic irradiation delivered by ^{131}I-labeled anti-CD45 antibody, combined with cyclophosphamide and total body irradiation. Blood 1995;85:1122–31.

12. Burke JM, Caron PC, Papadopoulos EB, et al. Cytoreduction with iodine-131-anti-CD33 antibodies before bone marrow transplantation for advanced myeloid leukemias. Bone Marrow Transplant 2003;32:549–56.

13. Bunjes D, Buchmann I, Duncker C, et al. Rhenium 188-labeled anti-CD66 (a, b, c, e) monoclonal antibody to intensify the conditioning regimen prior to stem cell transplantation for patients with high-risk acute myeloid leukemia or myelodysplastic syndrome: results of a phase I-II study. Blood 2001;98:565–72.

14. Appelbaum F, Matthews D, Eary JF, et al. The use of radiolabeled anti-CD33 antibody to augment marrow irradiation prior to marrow transplantation for acute myelogenous leukemia. Transplantation 1992;54:829–33.

15. Pagel JM, Appelbaum FR, Eary JF, et al. ^{131}I-anti-CD45 antibody plus busulfan and cyclophosphamide before allogeneic hematopoietic cell transplantation for treatment of acute myeloid leukemia in first remission. Blood 2006;107:2184–91.

16. Scheinberg DA, Lovett D, Divgi CR, et al. A phase I trial of monoclonal antibody M195 in acute myelogenous leukemia: specific bone marrow targeting and internalization of radionuclide. J Clin Oncol 1991;9:478–90.

17. Jurcic JG, DeBlasio T, Dumont L, Yao TJ, Scheinberg DA. Molecular remission induction with retinoic acid and anti-CD33 monoclonal antibody HuM195 in acute promyelocytic leukemia. Clin Cancer Res 2000;6:372–80.

18. Sgouros G, Ballangrud AM, Jurcic JG, et al. Pharmacokinetics and dosimetry of an α-particle emitter labeled antibody:213Bi-HuM195 (anti-CD33) in patients with leukemia. J Nucl Med 1999;40:1935–46.

19. van der Jagt RH, Badger CC, Appelbaum FR, et al. Localization of radiolabeled antimyeloid antibodies in a human acute leukemia xenograft tumor model. Cancer Res 1992;52:89–94.

20. Nakano A, Harada T, Morikawa S, Kato Y. Expression of leukocyte common antigen (CD45) on various human leukemia/lymphoma cell lines. Acta Pathol Jpn 1990;40:107–15.

21. Taetle R, Ostergaard H, Smedsrud M, Trowbridge I. Regulation of CD45 expression in human leukemia cells. Leukemia 1991;5:309–14.

22. Matthews DC, Badger CC, Fisher DR, et al. Selective radiation of hematolymphoid tissue delivered by anti-CD45 antibody. Cancer Res 1992;52:1228–34.

23. Axworthy DB, Reno JM, Hylarides MD, et al. Cure of human carcinoma xenografts by a single dose of pretargeted yttrium-90 with negligible toxicity. Proc Natl Acad Sci U S A 2000;97:1802–7.

24. Paganelli G, Grana C, Chinol M, et al. Antibody-guided three-step therapy for high grade glioma with yttrium-90 biotin. Eur J Nucl Med 1999;26:348–57.

25. Goodwin DA, Meares CF, Osen M. Biological properties of biotin-chelate conjugates for pretargeted diagnosis and therapy with the avidin/biotin system. J Nucl Med 1998;39:1813–8.

26. Sharkey RM, Karacay H, Richel H, et al. Optimizing bispecific antibody pretargeting for use in radioimmunotherapy. Clin Cancer Res 2003;9:3897–913S.

27. Zhang M, Zhang Z, Garmestani K, et al. Pretarget radiotherapy with an anti-CD25 antibody-streptavidin fusion protein was effective in therapy of leukemia/lymphoma xenografts. Proc Natl Acad Sci U S A 2003;100:1891–5.

28. Theodore L, Axworthy D. Cluster clearing agents. U.S. Patent 6,172,045; 2001.

29. Dubel S, Breitling F, Kontermann R, et al. Bifunctional and multimeric complexes of streptavidin fused to single chain antibodies (scFv). J Immunol Methods 1995;178:201–9.

30. Kipriyanov SM, Little M, Kropshofer H, et al. Affinity enhancement of a recombinant antibody: formation of complexes with multiple valency by a single-chain Fv fragment-core streptavidin fusion. Protein Eng 1996;9:203–11.

31. Schultz J, Lin Y, Sanderson J, et al. A tetravalent single-chain antibody-streptavidin fusion protein for pretargeted lymphoma therapy. Cancer Res 2000;60:6663–9.

32. Telleman P, Junghans RP. The role of the Brambell receptor (FcRB) in liver: protection of endocytosed immunoglobulin G (IgG) from catabolism in hepatocytes rather than transport of IgG to bile. Immunology 2000;100:245–51.

33. Yao Z, Zhang M, Axworthy DB, et al. Radioimmunotherapy of A431 xenografted mice with pretargeted B3 antibody-streptavidin and (90)Y-labeled 1,4,7,10-tetraazacyclododecane-*N,N',N'',N'''*-tetraacetic acid (DOTA)-biotin. Cancer Res 2002;62:5755–60.

34. Graves SS, Dearstyne E, Lin Y, et al. Combination therapy with pretarget CC49 radioimmunotherapy and gemcitabine prolongs tumor doubling time in a murine xenograft model of colon cancer more effectively than either monotherapy. Clin Cancer Res 2003;9:3712–21.

35. Knox SJ, Goris ML, Tempero M, et al. Phase II trial of yttrium-90-DOTA-biotin pretargeted by NR-LU-10 antibody/streptavidin in patients with metastatic colon cancer. Clin Cancer Res 2000;6:406–14.

36. Goshorn S, Sanderson J, Axworthy D, et al. Preclinical evaluation of a humanized NR-LU-10 antibody-streptavidin fusion protein for pretargeted cancer therapy. Cancer Biother Radiopharm 2001;16:109–23.

37. Ramm K, Pluckthun A. High enzymatic activity and chaperone function are mechanistically related features of the dimeric *E. coli* peptidyl-prolyl-isomerase FkpA. J Mol Biol 2001;310:485–98.

38. Sawyer JR, Schlom J, Kashmiri SV. The effects of induction conditions on production of a soluble anti-tumor sFv in *Escherichia coli*. Protein Eng 1994;7:1401–6.

39. Lindmo T, Boven E, Cuttitta F, Fedorko J, Bunn PA, Jr. Determination of the immunoreactive fraction of radiolabeled monoclonal antibodies by linear extrapolation to binding at infinite antigen excess. J Immunol Methods 1984;72:77–89.

40. Badger CC, Krohn KA, Bernstein ID. *In vitro* measurement of avidity of radioiodinated antibodies. Int J Radiat Appl Instrum Part B 1987;14:605–10.

41. Hylarides MD, Mallett RW, Meyer DL. A robust method for the preparation and purification of antibody/streptavidin conjugates. Bioconjug Chem 2001;12:421–7.

42. Pagel J, Hedin N, Subbiah K, et al. Comparison of anti-CD20 and anti-CD45 antibodies for conventional and pretargeted radioimmunotherapy of B-cell lymphomas. Blood 2003;101:2340–8.

43. Pagel JM, Lin Y, Hedin N, et al. Comparison of a tetravalent single-chain antibody-streptavidin fusion protein and an antibody-streptavidin chemical conjugate for pretargeted anti-CD20 radioimmunotherapy of B-cell lymphomas. Blood. In press 2006.

44. Press OW, Corcoran M, Subbiah K, et al. A comparative evaluation of conventional and pretargeted radioimmunotherapy of CD20-expressing lymphoma xenografts. Blood 2001;98:2535–43.

45. Forero A, Weiden PL, Vose JM, et al. Phase 1 trial of a novel anti-CD20 fusion protein in pretargeted radioimmunotherapy for B-cell non-Hodgkin lymphoma. Blood 2004;104:227–36.

46. Breitz HB, Weiden PL, Beaumier PL, et al. Clinical optimization of pretargeted radioimmunotherapy with antibody-streptavidin conjugate and ^{90}Y-DOTA-biotin. J Nucl Med 2000;41:131–40.

47. Subbiah K, Hamlin DK, Pagel J, et al. Comparative immunoscintigraphy, toxicity, and efficacy of conventional and pretargeted radioimmunotherapy in a CD20-expressing human lymphoma xenograft model. J Nucl Med 2003;44:437–45.

48. Hamblett KJ, Kegley BB, Hamlin DK, et al. A streptavidin-biotin binding system that minimizes blocking by endogenous biotin. Bioconjug Chem 2002;13:588–98.

A Genetically Engineered Anti-CD45 Single-Chain Antibody-Streptavidin Fusion Protein for Pretargeted Radioimmunotherapy of Hematologic Malignancies

Yukang Lin, John M. Pagel, Donald Axworthy, et al.

Updated version	Access the most recent version of this article at: http://cancerres.aacrjournals.org/content/66/7/3884

Cited articles	This article cites 46 articles, 25 of which you can access for free at: http://cancerres.aacrjournals.org/content/66/7/3884.full#ref-list-1
Citing articles	This article has been cited by 12 HighWire-hosted articles. Access the articles at: http://cancerres.aacrjournals.org/content/66/7/3884.full#related-urls

E-mail alerts	Sign up to receive free email-alerts related to this article or journal.
Reprints and Subscriptions	To order reprints of this article or to subscribe to the journal, contact the AACR Publications Department at pubs@aacr.org.
Permissions	To request permission to re-use all or part of this article, use this link http://cancerres.aacrjournals.org/content/66/7/3884. Click on "Request Permissions" which will take you to the Copyright Clearance Center's (CCC) Rightslink site.